Sharp peak of the critical current density in $BaFe_{2-x}Ni_xAs_2$ at optimal composition

Derrick Van Gennep,[1] Abdelwahab Hassan,[2] Huiqian Luo,[3,4] and Mahmoud Abdel-Hafiez[1,5,*]

[1]*Lyman Laboratory of Physics, Harvard University, Cambridge, Massachusetts 02138, USA*

[2]*Faculty of science, Physics department, Fayoum University, 63514-Fayoum, Egypt*

[3]*Beijing National Laboratory for Condensed Matter Physics, Institute of Physics, Chinese Academy of Sciences, Beijing 100190, China*

[4]*Songshan Lake Materials Laboratory, Dongguan, Guangdong 523808, China*

[5]*Department of Physics and Astronomy, Uppsala University, Box 516, SE-751 20 Uppsala, Sweden*

(Received 22 April 2020; revised manuscript received 23 May 2020; accepted 12 June 2020; published 25 June 2020)

The importance of type-II superconductors with strong pinning comes from their ability to carry large electrical currents in the presence of a magnetic field. We report on the results of the bulk magnetization measurements in the superconducting state in high-quality single crystals of $BaFe_{2-x}Ni_xAs_2$ at various doping levels ranging from the underdoped to the overdoped regimes. The zero-temperature superconducting critical current density J_c at optimal composition $x = 0.10$, where the superconducting transition temperature T_c reaches a maximum of 19.9(0.4) K, displays a pronounced sharp peak in the doping dependence. Thus the observed doping dependence of the critical current implies that pinning becomes stronger upon initial doping. In addition, the best pinning conditions are realized in the presence of structural and magnetic domains. Our results strongly suggest that the high J_c values are mainly due to collective (weak) pinning of vortices by dense microscopic point defects with some contribution from a strong pinning mechanism. The experimental results of the normalized J_c present a remarkably good agreement with the δl pinning theoretical curve, confirming that pinning in our samples originates from spatial variations of the charge carrier mean free path leading to small bundle vortex pinning by randomly distributed (weak) pinning centers for $H \parallel c$.

DOI: 10.1103/PhysRevB.101.235163

I. INTRODUCTION

Although many questions concerning microscopic electronic properties of the iron pnictides have been successfully addressed [1–4], their potential for application is less clear. High critical temperature, high critical current density, high upper critical field, and flux jumps are important factors for practical applications of superconductors; though all of these issues are also of great interest for fundamental research. The superconducting critical current density J_c is a measure of the strength of the pinning force density and can be very conveniently used to characterize the strength of disorder in the system. The J_c can be increased significantly by introducing artificial pinning centers. It depends on a complex interplay of individual pinning centers, the interaction between vortices, and thermal fluctuations [5–7]. One of the most relevant parameters in producing highly functional superconducting materials is the current-carrying capacity. The J_c of the iron pnictides usually display several regimes as a consequence of a pinning landscape with random point disorder and a low density of large defects [5,8]. J_c, depending on the disorder, either decreases monotonically or displays a second peak (SP) in the magnetization, also called a "fishtail"[9,10]. Interestingly, the existence of the SP is found to be doping-dependent [11]. Therefore understanding the superconducting J_c is a central issues pertaining to both fundamental science as well as technological applications.

The possibility to achieve a strong pinning of vortices and high critical current densities in Fe-based superconductors is very high due to the short coherence lengths in these materials. In type-II superconductors, above the lower critical field H_{c1}, the magnetic field (H) penetrates the bulk of a superconductor in the form of vortices (or fluxoids, each one bringing a quantized unit of magnetic field flux $\phi = hc/2e = 2.068 \times 10^{-7}$ G cm^2), and each vortex consists of a normal core surrounded by a whirlpool of supercurrent [12]. The motion of vortices is assisted by thermal fluctuations which can cause melting of the vortex lattice. The inclusion of thermal fluctuations in type-II superconductors also affects the vortex dynamical behavior, i.e., the vortex lines can move due to thermally activated jumps over the pinning barriers, leading to the famous creep phenomenon in type-II superconductors [13]. However, the J_c and vortex dynamics have been extensively studied for all families of Fe-pnictides and show reasonably high J_c at low temperature [8,14–25]. It turns out that the occurrence of the SP is generic to the $M(H)$ behavior in a variety of Fe-based superconductors. This feature has been observed in the Bi-based and Tl-based cuprate superconductors and the SP is found to be temperature

*mhafiez@g.harvard.edu

independent for Bi-based and Tl-based cuprate [26–28]. In Nb_3Sn and MgB_2 superconductors, the peak effect has been observed near the H_{c2} [29,30]. However, the electron and hole-doped Ca-122 materials as well as the isoelectronic substitution in the $BaFe_2As_{2-x}P_x$ system appear to be quite distinct in this regard as previous studies have shown an a SP to be surprisingly absent [31–34]. The appearance of a SP is believed to be directly associated with the nature of pinning and thereof with the vortex creep mechanism [35].

Understanding vortex motion in superconductors is important when considering their ability to carry electrical current. To get the clearest picture, conducting careful experiments on a clean superconductor, such as $BaFe_{2-x}Ni_xAs_2$, is highly valuable. The measurement of isothermal magnetization and the scaling behavior of the flux pinning forces, determined from the critical current densities, are the most extensively used tools to study the details of the underlying flux pinning mechanisms in a variety of superconducting materials. In this paper, we show the J_c, flux jump, and SP of high-quality single crystals in a electron-doped 122 Fe-pnictide material (see Ref. [36]) by means of a study of bulk magnetization with $H \parallel c$ axis. The corresponding electron and hole-doped Ba122 are well studied in terms of the above-mentioned properties [15,19,20,37–39]. A detailed study for vortex dynamics in $Ba(Fe_{0.93}Co_{0.07})_2As_2$ was done by Prozorov *et al.* [15]. They reported that the vortex dynamics can be explained by the collective creep theory in low temperature and low magnetic field region. Our analysis implies that high J_c is mainly due to collective (weak) pinning of vortices by dense microscopic point defects with some contribution from a strong pinning mechanism. In addition, we present evidence in favor of pinning related to spatial variations of the charge carrier mean free path leading to small bundle vortex pinning by randomly distributed (weak) pinning centers for $H \parallel c$. The critical current density J_c at optimal composition $x = 0.10$ displays a pronounced sharp peak in the doping dependence. The experimental results of the normalized J_c present a remarkably good agreement with the δl pinning theoretical curve.

II. EXPERIMENTAL

$BaFe_{2-x}Ni_xAs_2$ ($x = 0.065$, 0.085, 0,092, 0.096, 0.1, 0.12, and 0.15) single crystals, grown by a FeAs self-flux method. Details for the growth process and sample characterization were published elsewhere [40,41]. Magnetization measurements were performed using a Quantum Design SC quantum interference magnetometer along $H \parallel c$ up to $H = 9$ T.

III. RESULTS AND DISCUSSION

The field dependence of the isothermal magnetization M at various temperatures up to 9 T for $H \parallel c$, and for $x = 0.10$, 0.092, and 0.15 is presented in Figs. 1(a)–1(c), respectively. Irregular jumps close to $H = 0$ are presented in the $M(H)$ for $x = 0.092$ and 0.10 at $T = 2$ K. Interestingly, for both samples, this irregular jump occurs only in the virgin branch of the $M(H)$ curves and no such feature was found in other magnetic field branches. Figures 1(d)–1(f) present the field dependence of the isothermal magnetization M at various temperatures very close to T_c up to 9 T, for $x = 0.10$, 0.092, and 0.15,

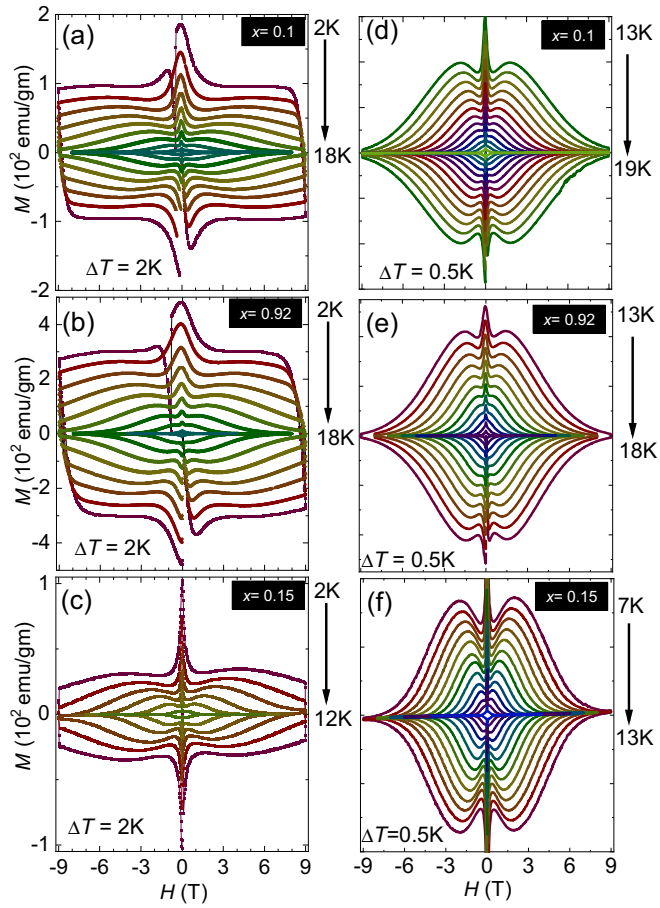

FIG. 1. [(a)–(c)] Magnetic field dependence of the isothermal magnetization M vs H loops measured at different temperatures ranging from 2 to 18 K for $x = 0.1$ and 0.92 and from 2 to 12 K for $x = 0.1$ up to 90 kOe for each 2-K temperature interval with the field parallel to the c axis. (d) 13–19 K for each 0.5 K, (e) 13–18 K for each 0.5 K, and (f) 7–13 K for each 0.5 K, plots at high temperatures exhibit a pronounced second peak for $x = 0.10$, 0.092, and 0.15, respectively.

respectively. The superconducting $M(H)$ exhibits no magnetic background, indicating that our samples contain negligible amounts of magnetic impurities. From the hysteresis loops in $M(H)$, we have extracted the magnetic field dependence of the critical current density J_c for the investigated single crystals at different temperatures, exploiting the critical state model with the assumption of field-independent J_c. To deduce the J_c values, we used the Bean mode [42]:

$$J_c = \frac{20\Delta M}{\left[a\left(1 - \frac{a}{3b}\right)\right]}, \tag{1}$$

where $\Delta M = M_{dn} - M_{up}$, M_{dn}, and M_{up} are the magnetization measured with decreasing and increasing applied field, respectively, a (cm) and b (cm) are sample widths ($a < b$). The unit of ΔM is in electromagnetic unit per cubic centimeter and the calculated J_c is in ampere per square centimeter. Figure 2 presents the calculated J_c for various temperatures for $x = 0.1$ in (a), 0.092 in (b). J_c curves also show a SP and decrease monotonically with field, which is similar to the magnetization data [36]. Figure 1(c) presents the field dependence of the isothermal magnetization M at various temperatures very

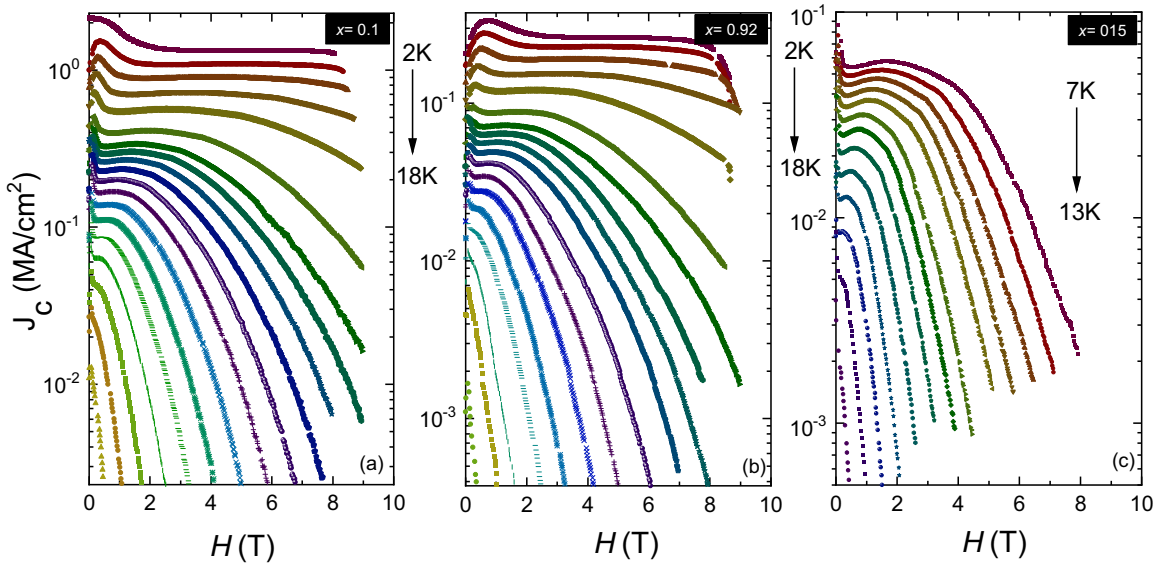

FIG. 2. Critical current density vs magnetic field for the field applied along the c axis for $x = 0.1$ in (a), 0.092 in (b), and 0.15 in (c).

close to T_c up to 9 T for $H \parallel c$ for $x = 0.15$. In addition, the SC $M(H)$ exhibits no magnetic background. It is apparent that our investigated samples contain negligible magnetic impurities due to the absence of magnetic background in all studied samples. The width of the magnetic loops decrease while increasing the applied field. However, at higher temperatures the width of the loops initially decreases showing a minimum at the H_m field and then increases again. Further, the $M(H)$ loops demonstrate the SP, mentioned above. The SP effect has been studied extensively and its origin may be attributed to various mechanisms. It has been well established that the SP effect is strongly influenced by the oxygen deficiency in cuprates [43,44]. In the case of Fe-based superconductors, the local magnetic moments may form the small size normal cores, and may be a possible reason of the SP effect [16]. However, the real pinning mechanism needs further investigation. The position of the SP shifts to higher fields while decreasing temperature, eventually beyond the available field range. This can explain the nonvisibility of a SP at low temperatures in the Fig. 2. The $M(H)$ loops show irreversibility in magnetization, which vanishes above a characteristic field $H_{\rm irr}$ (Fig. 1). Interestingly, the SP exhibits a pronounced doping dependence with values are comparable with Ba-122 superconductors [8,15–17,32]. This high J_c indicates strong pinning in our system.

Figure 3 (upper panel) presents the electronic phase diagram of $BaFe_{2-x}Ni_xAs_2$, which was obtained from magnetic and specific heat data. As can be seen that the magnetic and structural transitions coincide in the parent compound [$T_S(T_N)$ = 137(2) K] and then shows a suppression of the magnetic (T_N) and structural (T_S) phase transitions with increasing Ni concentration and the appearance of the SC transitions (see Refs. [36,45]). In addition, we have very recently shown that the superconducting gap in the nearly optimally doped compounds (coexistence with spin-density wave) is nodeless [36]. Interestingly, it has been shown that the magnetic order in 122 pnictides has preferential direction in the *ab* plane and is rigidly correlated with the orthorhombic axes [46]. Thus structural domains are the root of the magnetic domains. In this context, both structural and magnetic domains are clearly quite close to the optimal concentration, so that superconductivity coexists in the presence of both types of order.

Let us turn, then, to one of the main results, i.e., the general picture that can be obtained for the critical current density in $BaFe_{2-x}Ni_xAs_2$ system. The evolution of the superconducting critical current density taken for all doping levels presents a pronounced sharp peak at optimal composition in $J_c(x)$, Fig. 3 (bottom panel). However, even before, similar results were reported for the $Ba(Fe_{1-x}Co_x)_2As_2$ [15] and for the $Ca(Fe_{1-x}Co_x)_2As_2$ [32] systems. There is a clear asymmetry of J_c with respect to the $T_c(x)$ dome. As a function of doping, the critical current density starts to rise with increasing x until the optimal composition ($x = 0.10$). Below that, the J_c decreases with decreasing x. The possibility of enhancement of the J_c is due to an increase in intrinsic pinning arising from the domain walls of the coexisting AFM/orthorhombic phase. Thus observed doping dependence of the critical current imply that pinning becomes stronger upon initial doping. Furthermore, the best pinning conditions are realized in the presence of structural domains and the presence of magnetism. Therefore, the structural and magnetic domains play an important role and act as effective extended pinning centers which upon suppression of the related ordering phenomena by doping become more fine and intertwined, thus giving rise to enhanced J_c when increasing x in the underdoped regime.

However, one can argue that the observed enhancement is simply due to more robust superconductivity at the optimal composition. To address this argument, let us consider two samples with almost similar T_c on two sides of the peak around the optimal doping. For instance, for $x = 0.085$ and 0.15, whereas the slightly overdoped $x = 0.015$ with even higher $T_c \approx = 14$ K, the critical current is substantially lower. Clearly one can see from the comparison of the isothermal magnetization loops up to 9 T in the inset of bottom panel in Fig. 3, that difference between the samples is not due the effective magnetic field. In addition, the $M(H)$ loops for the

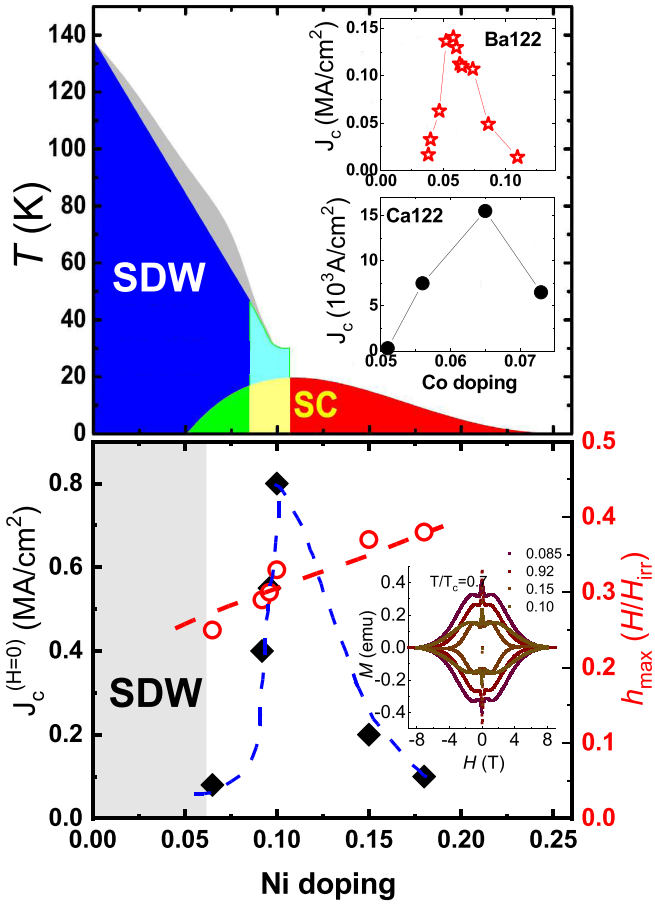

FIG. 3. Top panel presents the electronic phase diagram of $BaFe_{2-x}Ni_xAs_2$, showing the suppression of the magnetic (T_N) and structural (T_S) phase transitions with increasing Ni concentration and the appearance of the SC transitions (see Ref. [36]). The structural T_s and magnetic T_m transitions split with the increasing Ni doping. Insets in the top panel show the doping dependence of the critical current density of Co-doped in $BaFe_{2-x}Co_xAs_2$ [15] and $CaFe_{2-x}Co_xAs_2$ [32]. The bottom panel shows the evolution of the superconducting critical current density. The critical current was evaluated from the magnetic measurements, see Fig. 2. The right side represents the doping dependence of the reduced field H/H_{irr}.

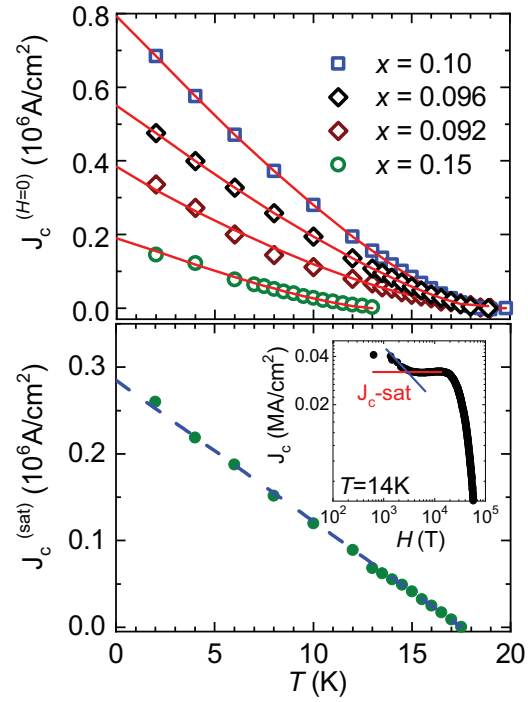

FIG. 4. The top panel presents the temperature dependence of supercurrent density for $BaFe_{2-x}Ni_xAs_2$. The critical current densities, calculated from Eq. (1), at $H \approx 0$ are represented by circles and those in the high-field saturated state (depicted in the bottom panel of the inset) are represented by squares. The red lines are a fit to the data using the function $J_c(T) = J_c(0)(1 - T/Tc)^n$. The blue dashed line in the bottom panel is a linear fit to the data. The inset shows a log-log plot of critical current density versus field at 14 K for $x = 0.10$.

samples show a very similar shape. Thus another reason for the enhancement of J_c should be investigated. Comparison of the top and bottom panels of Fig. 3 suggests that the critical current peaks in the underdoped regime, in which structural and magnetic orders still exist. It has been well reported in the $Ba(Fe_{1-x}Co_x)_2As_2$ system that moving toward finer and denser domain structures will both increase the pinning potential and introduce more pinning centers per unit volume [8]. Such natural linear defects extend along the c axis, known to occur in the 122 family of pnictide superconductors, create the defects of this type close to the optimal composition. Furthermore, the contribution of the magnetic order, which requires reduced symmetry from the orthorhombic distortion, may also be very important for pinning, as suggested by the data in the bottom panel of Fig. 3. On the other hand, clearly one can see that in Fig. 3 the sharp peak of the J_c is noticed where the x dependence of T_c is maximum, at the optimal doping.

In order to present the temperature dependence of the J_c, we have plotted J_c versus T in Fig. 4 for various Ni concentrations, and with $H \parallel c$. As is evident, the J_c decreases monotonically with increasing temperature. Similarly, with the sister compound $Ba(Fe_{0.93}Co_{0.07})_2As_2$ [15], we used the common function: $J_c = J_c(0)(1 - T/T_c)^n$ to fit our investigated data (red solid lines in Fig. 4) over the full temperature range. In contrast to $Ba_{0.65}Na_{0.35}Fe_2As_2$, in $PrFeAsO_{0.9}$ and $NdFeAsO_{0.9}F_{0.1}$ [8,23], the measured J_c exhibits a change in temperature dependence and cannot fit their data in the full temperature range with one function. The authors attributed this to an additive effect of weak collective pinning by dopant atoms and strong pinning by a spatial variation in dopant atom density. Beek *et al.* have investigated the possible sources for the size of the strong pinning and have shown that the strong pinning for 1111 compounds is caused by weak superconducting regions arising from dopant density variation [8]. For our investigated samples, the presented Ni concentration is determined by the inductively coupled plasma (ICP) analysis, where the real Ni composition is about 80% of the nominal value x (Ref. [40]). Note that our T_c is sensitive to Ni concentration in this series [40]. The Ni distribution could give rise to several nanometer size weak superconducting regions responsible for strong pinning. However, the present

series $BaFe_{2-x}Ni_xAs_2$ is different compared to the Beek *et al.* studies (1111 system) and the basic parameters such as coherence length and penetration length are lacking, which does not allow us to estimate the pinning characteristics. In addition, the signature of strong pinning has been reported for various Fe-based superconductors on high-quality single crystals [8,21,23,31].

In type-II superconductors, the low-field regime presents a weaker temperature dependence and the strong pinning is more active than the weak collective pinning [13]. The signature of strong pinning is evident in the field dependence of J_c, i.e., at low field $J_c(H)$ shows a plateau which is followed by a steep decrease of power-law behavior ($J_c \propto H^g$, $0.5 < g < 0.63$ [47,48]. In order to check for the presence of strong pinning in our system, we plotted J_c versus H at different temperatures, and estimated the exponent g. The inset of the bottom panel in Fig. 3 presents a log-log plot of critical current density versus field at 14 K for $x = 0.10$. With increasing field, it is observed that initially $J_c(H)$ exhibits a plateau, then decreases and at higher field it almost saturates at a value J_c-sat, which is comparable to the strong pinning model reported in [47,48]. The bottom panel in Fig. 3 summarized the temperature variation of J_c-sat and shows linear behavior. Interestingly, these observations illustrate the presence of strong pinning in our investigated system, while the major contribution to Jc comes from weak collective pinning, as previously observed in $PrFeAsO_{0.9}$, $NdFeAsO_{0.9}F_{0.1}$ and $BaFe_2(As_{1-x}P_x)_2$ families [8,21].

The critical current density J_c is always limited by the depairing current density $J_0 = 4B_c/3\sqrt{6}\mu_0\lambda$, where B_c and λ are the thermodynamic critical field and the Ginzburg-Landau penetration depth, respectively [49]. Therefore an interesting piece of information can be extracted from the ratio J_c/J_0. It should be noting that the pinning in low-temperature superconductors is usually strong ($J_c/J_0 \approx 10^{-2}$ to 10^{-1}) which comes from the interaction of vortices with extended defects [13], such as grain boundaries. On the other hand, for high T_c superconductors, i.e., the cuprate family, pinning is usually weak ($J_c/J_0 \approx 10^{-3}$ to 10^{-2}), normally arising from point defects, e.g., oxygen vacancies.

Let us turn now to the pinning force (F_p) in order to shed light on the mechanisms that rule pinning in the $BaFe_{2-x}Ni_xAs_2$ system. We have calculated the F_p from the critical current density and applied field, using $F_p = H \times J_c$ at different temperatures. The pinning force curves versus H obtained at different temperatures for a large variety of low-T_c and high-T_c superconductors can be scaled into a unique curve if they are plotted as a function of the reduced field, $h = H/H_{irr}$ [50–52]. Correspondingly, the theoretical Fp versus h curves present a maximum at different values of h. It has been well reported by Dew-Hughes [51] that in the scenario of a single vortex pinning mechanism, the normalized pinning force $f_p = F_p/F_p^{max}$ as a function of reduced field H/H_{irr}, where H_{irr} is the irreversible magnetic field and obtained from the zero value of T_c in T_c-H curves, depends on a scaling relation: $F_p \propto h^p(1-h)^q$, where $h = H/H_{irr}$, p and q are the exponents. The position of the peak and the extracted fitting parameters p and q provide information about the origin and the nature of pinning. To carefully study the F_p plot, we have measured more systematically $M(H)$ at various temperatures

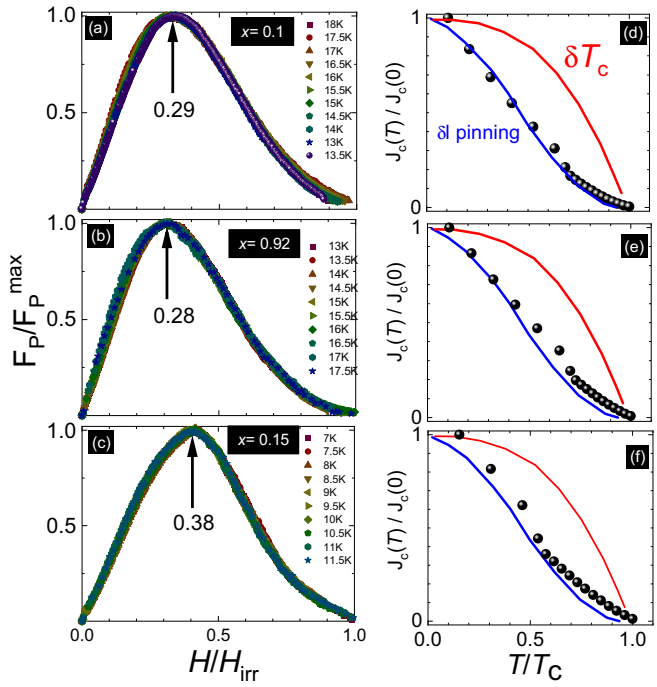

FIG. 5. Normalized flux pinning force $f_p = F_p/F_p^{max}$ shown as a function of reduced field H/H_{irr} at various temperatures for $x = 0.1$ in (a), 0.092 in (b), and 0.15 (c). (d)–(f) present the normalized critical current density at zero magnetic field $J_c(T)/J_c(0)$ as a function of reduced temperature T/T_c for $x = 0.1$ in (d), 0.092 in (e), and 0.15 (f). The solid lines are the same dependence plotted following a theoretical prediction for δT_c and δl pinning (see the text).

for all the studied samples. The main panel of Figs. 5(a)–5(c) show that a reasonably nice scaling of the data is observed at temperatures close to T_c. The obtained $J_c(0)$, h_{max}, and n values are summarized in Table I.

Generally, the different contributions to flux pinning in type-II superconductors are usually catalogued into two main categories δT_c (or δk) and δl (or normal) [13]. The δl-type pinning arises from a spatial variation in the mean free path of charge carriers and the defects are small and point sized. The δT_c-type pinning is caused by a spatial variation of the Ginzburg parameter k due to fluctuations in the critical temperature and the defects being larger than the coherence length [13,51]. In addition, it should be mentioned that the pinning centers are also classified as a function of the number of dimensions that are large with respect to the intervortex distance $d \approx (\Phi_0/B)^{0.5}$ [13,51]. The maximum of the $Fp(h)$

TABLE I. T_c, n obtained by fitting: $J_c(T) = J_c(0)(1 - T/Tc)^n$, parameters obtained by fitting: $F_p/F_pm^{ax} = A(h^p)(1 - h)^q$ to the experimental curves F_p/F_pm^{ax} vs h, where $h = H/H_{irr}$ and the superconducting critical current density $J_c^{(H=0)}$ (10^6 A C^{-1} m^{-2}).

Ni doping	T_c (K)	n	A	P	q	h	$J_c^{(H=0)}$
$x = 0.10$	19.9	1.55	25	1.49	3.9	2.9	0.8
$x = 0.092$	18.6	1.35	17	1.3	3.6	2.8	0.4
$x = 0.15$	8.4	1.28	35	1.6	3.8	0.38	0.19

curve is expected at higher h values in the case of δT_c pinning. According to the Dew-Hughes model, [51] for $h_{max} < 0.5$ indicates a δl-type pinning while $h_{max} > 0.5$ indicates δT_c-type pinning. Therefore, low values of $h_{max} < 0.5$ in the studied superconducting samples (see the right side in the bottom panel in Fig. 2) suggest that pinning is due to the presence of a large density of point-like defect centers whose dimensions are smaller than the intervortex distance in the investigated field range, which is similar to the results in Refs. [16,23]. However, the various values of h for different Ni compositions suggest that a contribution to pinning coming from surface pinning cannot be excluded. Therefore important information on the nature of the pinning mechanisms in type-II superconductors can be achieved by analyzing the scaled $F_p(h)$ curves.

The analysis of the scaled pinning force curves in the frame of the Dew-Hughes model revealed important information about pinning in type-II superconductors [13,51]. Using the temperature dependence of the zero field critical current density, we have further confirmed the nature of pinning. It has been predicted that the normalized critical current density $J_c(T)/J_c(0)$ exhibits different dependence on the reduced temperature for both δT_c and δl types of pinning, which the relation follows Eq. (2) for δT_c and Eq. (3) for δl types of pinning:

$$J_c(T)/J_c(0) = [1 - (T/T_c)^2]^{7/6}[1 - (T/T_c)^2]^{5/6}, \quad (2)$$

$$J_c(T)/J_c(0) = [1 - (T/T_c)^2]^{5/2}[1 - (T/T_c)^2]^{-1/2}. \quad (3)$$

Such dependence, along with the experimental data for the investigated crystals, is plotted in the inset of Figs. 4(a)–4(c) where $J_c(0)$ has been estimated from extrapolation of the $J_c(T)$ plot at $T/T_c = 0$. It is clearly seen from the insets in Fig. 4 that the pinning mechanism of our studied crystals is very close to the δl-types of pinning rather than to the δT_c-types of pinning. Indeed, we have obtained that, with varying $J_c(0)$, the $J_c(T)/J_c(0)$ for our three superconducting samples closely approaches that for δl-type pinning, both in terms of shape and value.

In summary, we have measured the isothermal magnetization loops in single crystalline samples of the hole-doped Fe-pnictide $BaFe_{2-x}Ni_xAs_2$. The $M(H)$ loops exhibit a so-called fishtail anomaly (or a second peak, SP), which is easily observable up to temperatures close to T_c. In addition, remarkable flux jumps are observed at low temperatures. The critical current densities J_c calculated from the $M(H)$ loops are reasonably high and agree well with other electron-doped 122 compounds. The zero-temperature superconducting critical current density J_c at optimal composition $x = 0.10$, where the superconducting transition temperature T_c reaches a maximum, displays a pronounced sharp peak in the doping dependence. Thus the observed doping dependence of the critical current implies that pinning becomes stronger upon initial doping. The analysis of temperature- and field-dependent J_c indicates that collective (weak) pinning of vortices by dense microscopic point defects is mainly responsible for the large values of J_c, though a strong pinning mechanism is also likely to give some contribution. The experimental results of the normalized J_c present a remarkably good agreement with the δl pinning theoretical curve, confirming that pinning in our samples originates from spatial variations of the charge carrier mean free path leading to small bundle vortex pinning by randomly distributed (weak) pinning centers for $H \parallel c$. Our results emphasize the importance of chemical tuning for recognizing the application potential of the $BaFe_{2-x}Ni_xAs_2$ superconductor.

ACKNOWLEDGMENTS

We appreciate the useful discussions with Christoph Geibel, Alexander Vasiliev, and Rüdiger Klingeler. M.A.-H. would like to acknowledge the support from the Swedish Research Council (VR) and from AGYA [53]. A.H. thanks the support from STDF (Egypt). H.L. acknowledge the support from the National Key Research and Development Program of China (Grant No. 2018YFA0704200), the National Natural Science Foundation of China (Grants No. 11822411 and No. 11961160699), the Strategic Priority Research Program (B) of the Chinese Academy of Sciences (CAS) (Grants No. XDB07020300 and No. XDB25000000), and the Youth Innovation Promotion Association of CAS (Grant No. 2016004).

[1] R. M. Fernandes and A. V. Chubukov, Rep. Prog. Phys. **80**, 014503 (2017).
[2] Y. Wang, W. Hu, R. Yu, and Q. Si, Phys. Rev. B **100**, 100502(R) (2019).
[3] X. Lu, J. T. Park, R. Zhang, H. Luo, A. H. Nevidomskyy, Q. Si, and P. Dai, Science **345**, 657 (2014).
[4] J. Paglione and R. L. Greene, Nat. Phys. **6**, 645 (2010).
[5] N. Haberkorn, M. Xu, W. R. Meier, J. Schmidt, S. L. Budko, and P. C. Canfield, Phys. Rev. B **100**, 064524 (2019).
[6] R. Willa, A. E. Koshelev, I. A. Sadovskyy, and A. Glatz, Phys. Rev. B **98**, 054517 (2018).
[7] H. Hosono, A. Yamamoto, H. Hiramatsu, and Y. Ma, Mater. Today **21**, 278 (2018).
[8] C. J. van der Beek, G. Rizza, M. Konczykowski, P. Fertey, I. Monnet, T. Klein, R. Okazaki, M. Ishikado, H. Kito, A. Iyo, H. Eisaki, S. Shamoto, M. E. Tillman, S. L. Budko, P. C. Canfield, T. Shibauchi, and Y. Matsuda, Phys. Rev. B **81**, 174517 (2010).
[9] R. Prozorov, N. Ni, M. A. Tanatar, V. G. Kogan, R. T. Gordon, C. Martin, E. C. Blomberg, P. Prommapan, J. Q. Yan, S. L. Budko, and P. C. Canfield, Phys. Rev. B **78**, 224506 (2008).
[10] Y. Nakajima, Y. Tsuchiya, T. Taen, T. Tamegai, S. Okayasu, and M. Sasase, Phys. Rev. B **80**, 012510 (2009).
[11] Y. Liu, L. Zhou, K. Sun, W. E. Straszheim, M. A. Tanatar, R. Prozorov, and T. A. Lograsso, Phys. Rev. B **97**, 054511 (2018).
[12] M. Tinkham, *Introduction to Superconductivity* (McGraw-Hill, New York, 1996).
[13] G. Blatter, M. V. Feigel'man, V. B. Geshkenbein, A. I. Larkin, and V. M. Vinokur, Rev. Mod. Phys. **66**, 1125 (1994).
[14] P. J. Moll, R. Puzniak, F. Balakirev, K. Rogacki, J. Karpinski, N. D. Zhigadlo, and B. Batlogg, Nat. Mater. **9**, 628 (2010).

[15] R. Prozorov, M. A. Tanatar, N. Ni, A. Kreyssig, S. Nandi, S. L. Budko, A. I. Goldman, and P. C. Canfield, Phys. Rev. B **80**, 174517 (2009).
[16] H. Yang, H. Luo, Z. Wang, and H.-H. Wen, Appl. Phys. Lett. **93**, 142506 (2008).
[17] D. L. Sun, Y. Liu, and C. T. Lin, Phys. Rev. B **80**, 144515 (2009).
[18] Xiao-Lin Wang, S. R. Ghorbani, Sung-Ik Lee, S. X. Dou, C. T. Lin, T. H. Johansen, K.-H. Müller, Z. X. Cheng, G. Peleckis, M. Shabazi, A. J. Qviller, V. V. Yurchenko, G. L. Sun, and D. L. Sun, Phys. Rev. B **82**, 024525 (2010).
[19] R. Kopeliansky, A. Shaulov, B. Ya. Shapiro, Y. Yeshurun, B. Rosenstein, J. J. Tu, L. J. Li, G. H. Cao, and Z. A. Xu, Phys. Rev. B **81**, 092504 (2010).
[20] B. Shen, P. Cheng, Z. Wang, L. Fang, C. Ren, L. Shan, and H.-H. Wen, Phys. Rev. B **81**, 014503 (2010).
[21] C. J. van der Beek, M. Konczykowski, S. Kasahara, T. Terashima, R. Okazaki, T. Shibauchi, and Y. Matsuda, Phys. Rev. Lett. **105**, 267002 (2010).
[22] A. K. Pramanik, L. Harnagea, C. Nacke, A. U. B. Wolter, S. Wurmehl, V. Kataev, and B. Büchner, Phys. Rev. B **83**, 094502 (2011).
[23] A. K. Pramanik, S. Aswartham, A. U. B. Wolter, S. Wurmehl, V. Kataev, and B. Büchner, J. Phys.: Condens. Matter **25**, 495701 (2013).
[24] M. Abdel-Hafiez, J. Ge, A. N. Vasiliev, D. A. Chareev, J. Van de Vondel, V. V. Moshchalkov, and A. V. Silhanek, Phys. Rev. B **88**, 174512 (2013).
[25] B. Maiorov, T. Katase, S. A. Baily, H. Hiramatsu, T. G. Holesinger, H. Hosono., and L. Civale, Supercond. Sci. Technol. **24**, 055007 (2011).
[26] A. Piriou, E. Giannini, Y. Fasano, C. Senatore, and Ø. Fischer, Phys. Rev. B **81**, 144517 (2010).
[27] G. Yang, P. Shang, S. D. Sutton, I. P. Jones, J. A. Abell, and C. E. Gough, Phy. Rev. B **48**, 4054 (1993).
[28] V. Hardy, A. Wahl, A. Ruyter, A. Maignan, C. Martin, L. Coudrier, J. Provost, and Ch. Simon, Physica C **232**, 347 (1994).
[29] R. Lortz, N. Musolino, Y. Wang, A. Junod, and N. Toyota, Phys. Rev. B **75**, 094503 (2007).
[30] M. Pissas, S. Lee, A. Yamamoto, and S. Tajima, Phys. Rev. Lett. **89**, 097002 (2002).
[31] N. Haberkorn, B. Maiorov, M. Jaime, I. Usov, M. Miura, G. F. Chen, W. Yu, and L. Civale, Phys. Rev. B **84**, 064533 (2011).
[32] A. K. Pramanik, L. Harnagea, S. Singh, S. Aswartham, G. Behr, S. Wurmehl, C. Hess, R. Klingeler, and B. Büchner, Phys. Rev. B **82**, 014503 (2010).
[33] M. Abdel-Hafiez, P. J. Pereira, S. A. Kuzmichev, T. E. Kuzmicheva, V. M. Pudalov, L. Harnagea, A. A. Kordyuk, A. V. Silhanek, V. V. Moshchalkov, B. Shen, H. H. Wen, A. N. Vasiliev, and X. J. Chen, Phys. Rev. B **90**, 054524 (2014).
[34] S. V. Chong, S. Hashimoto, and K. Kadowaki, Solid State Commun. **150**, 1178 (2010).
[35] D. Giller, A. Shaulov, R. Prozorov, Y. Abulafia, Y. Wolfus, L. Burlachkov, Y. Yeshurun, E. Zeldov, V. M. Vinokur, J. L. Peng, and R. L. Greene, Phys. Rev. Lett. **79**, 2542 (1997).
[36] M. Abdel-Hafiez, Y. Zhang, Z. He, J. Zhao, C. Bergmann, C. Krellner, C-G. Duan, X. Lu, H. Luo, P. Dai, and X-J. Chen, Phys. Rev. B **91**, 024510 (2015).
[37] Y. Nakajima, T. Taen, and T. Tamegai, J. Phys. Soc. Jpn. **78**, 023702 (2009).
[38] A. Yamamoto, J. Jaroszynski, C. Tarantini, L. Balicas, J. Jiang, A. Gurevich, D. C. Larbalestier, R. Jin, A. S. Sefat, M. A. McGuire, B. C. Sales, D. K. Christen, and D. Mandrus, Appl. Phys. Lett. **94**, 062511 (2009).
[39] M. R. Eskildsen, L. Ya. Vinnikov, I. S. Veshchunov, T. M. Artemova, T. D. Blasius, J. M. Densmore, C. D. Dewhurst, N. Ni, A. Kreyssig, S. L. Budko, P. C. Canfield, and A. I. Goldman, Physica C **469**, 529 (2009).
[40] Y. C. Chen, X. Y. Lu, M. Wang, H. Q. Luo, and S. L. Li, Supercond. Sci. Technol. **24**, 065004 (2011).
[41] H. Luo, X. Lu, R. Zhang, M. Wang, E. A. Goremychkin, D. T. Adroja, S. Danilkin, G. Deng, Z. Yamani, and P. Dai, Phys. Rev. B **88**, 144516 (2013).
[42] C. P. Bean, Phys. Rev. Lett. **8**, 250 (1962).
[43] M. Daeumling, J. M. Seuntjens, and D. C. Larbalestier, Nature (London) **346**, 332 (1990).
[44] L. Krusin-Elbaum, L. Civale, V. M. Vinokur, and F. Holtzberg, Phys. Rev. Lett. **69**, 2280 (1992).
[45] X. Lu, H. Gretarsson, R. Zhang, X. Liu, H. Q. Luo, W. Tian, M. Laver, Z. Yamani, Y. J. Kim, A. H. Nevidomskyy, Q. Si, and P. Dai, Phys. Rev. Lett. **110**, 257001 (2013).
[46] Y. Su, P. Link, A. Schneidewind, Th. Wolf, P. Adelmann, Y. Xiao, M. Meven, R. Mittal, M. Rotter, D. Johrendt, Th. Brueckel, and M. Loewenhaupt, Phys. Rev. B **79**, 064504 (2009).
[47] C. J. van der Beek, M. Konczykowski, A. Abal'oshev, I. Abal'oshev, P. Gierlowski, S. J. Lewandowski, M. V. Indenbom, and S. Barbanera, Phys. Rev. B **66**, 024523 (2002).
[48] Yu N. Ovchinnikov and B. I. Ivlev, Phys. Rev. B **43**, 8024 (1991).
[49] R. Griessen, Wen Hai-hu, A. J. J. van Dalen, B. Dam, J. Rector, H. G. Schnack, S. Libbrecht, E. Osquiguil, and Y. Bruynseraede, Phys. Rev. Lett. **72**, 1910 (1994).
[50] M. R. Koblischka, A. J. J. van Dalen, T. Higuchi, S. I. Yoo, and M. Murakami, Phys. Rev. B **58**, 2863 (1998).
[51] D. Dew-Hughes, Phil. Mag. **30**, 293 (1974).
[52] W. A. Fietz and W. W. Webb, Phys. Rev. **178**, 657 (1969).
[53] www.agya.info.